JOURNAL OF THE MECHANICAL BEHAVIOR OF BIOMEDICAL MATERIALS 35 (2014) 132–143

Available online at www.sciencedirect.com

ScienceDirect

www.elsevier.com/locate/jmbbm

Research Paper

Characterization of biomechanical properties of agar based tissue mimicking phantoms for ultrasound stiffness imaging techniques

Kavitha Manickam[a,*], *Ramasubba Reddy Machireddy*[a], *Suresh Seshadri*[b]

[a]*Biomedical Engineering Group, Department of Applied Mechanics, IIT Madras, Chennai 600 036, India*
[b]*Mediscan Systems, Chennai 600 004, India*

ARTICLE INFO

Article history:
Received 22 November 2013
Received in revised form
22 March 2014
Accepted 25 March 2014
Available online 1 April 2014

Keywords:
Tissue mimicking phantoms
Agar
Stiffness imaging
Elastic
Viscoelastic
Hyperelastic

ABSTRACT

Pathological changes of the body have been observed to change the mechanical properties of soft tissue types which can be imaged by ultrasound elastography. Though initial clinical results using ultrasound elastography in detection of tumors are promising, quantification of signal to noise ratio, resolution and strain image patterns are the best achieved under a controlled study using phantoms with similar biomechanical properties of normal and abnormal tissues. The purpose of this work is to characterize the biomechanical properties of agar based tissue mimicking phantoms by varying the agar concentration from 1.7 to 6.6% by weight and identify the optimum property to be used in classification of cancerous tissues. We performed quasi-static uniaxial compression test under a strain rate of 0.5 mm/min up to 15% strain and measured Young's modulus of phantom samples which are from 50 kPa to 450 kPa. Phantoms show nonlinear stress–strain characteristics at finite strain which were characterized using hyperelastic parameters by fitting Neo-Hookean, Mooney Rivlin, Ogden and Veronda Westmann models. We also investigated viscoelastic parameters of the samples by conducting oscillatory shear rheometry at various precompression levels (2–5%). Loss modulus values are always less than storage modulus which represents the behavior of soft tissues. The increase in agar concentration increases the shear modulus of the samples as well as decreases the linear viscoelastic region. The results suggest that dynamic shear modul are more promising than linear and nonlinear elastic modul in differentiation of various classes of abnormal tissues.

*Corresponding author.
E-mail address: kavitharunkumar@gmail.com (K. Manickam).

http://dx.doi.org/10.1016/j.jmbbm.2014.03.017
1751-6161/

1. Introduction

In clinical examinations of breast and prostate, clinicians use palpation to detect abnormalities in tissue. Invasive Ductal Carcinomas (a malignant breast cancer) and prostate cancer tissues are stiffer than normal breast and prostate tissues (Krouskop et al., 1998). In general, changes in tissue stiffness are highly correlated with pathological changes (Skovoroda et al., 1995). Over the last 20 years, stiffness imaging techniques have been developed to assess the stiffness properties of tissues in vivo. These methods basically involve applying a mechanical excitation to tissues of interest and measuring tissue deformation. Stiff tissues show less deformation than softer tissues under compression or shear. Thus by estimating tissue deformation induced by compression or shear, tissue strain information can be obtained. The measured deformation can be displayed directly as an image or strain is computed and displayed as a gray scale map known as elastogram (Ophir, 1991). Ultrasound elastography is one such stiffness imaging technique where the compression is given by probe and tissue deformation is imaged using ultrasound pulses. Based on the tissue strain to be analyzed, elastography could be further grouped into two major categories namely conventional linear elastography and nonlinear elastography (Samani et al., 2003).

In conventional elastography, tissue is stimulated by applying very low frequency excitation (quasi-static compression). Due to this reason, it is assumed to exhibit linear elastic behavior and using Hooke's law, tissue elastic behavior is characterized with only one parameter i.e. Young's modulus. In isotropic materials, the ratio of longitudinal deformation which is in the direction of applied load (strain) in response to an applied longitudinal force (stress) is known as Young's modulus (E) of elasticity. The shear modulus (G) relates transverse strain to transverse stress and bulk modulus (K) describes the change in volume of a material to external stress. Poisson's ratio is the ratio of transverse strain to longitudinal strain. These parameters are interrelated so that the knowledge of any two allows the estimation of other two. On the other hand, most of the tissues like breast and liver, even for a very small compression (less than 10%), deform significantly. Cancer tissue is not only much (2–10 times) stiffer than fat and normal glandular tissues but also displays much more nonlinear increase in stiffness (Krouskop et al., 1998). While normal tissues and cancerous tissues have similar elastic moduli at small strain (less than 10%), their moduli at larger strain (above 10%) differ by 2–3 order of magnitudes. Thus while it might not be possible to distinguish malignant tumors from benign lesions at small strain alone, it may be possible to do this by considering data at larger strain. Over a wide deformation range, Young's modulus cannot be assumed as a constant and may not be sufficient to represent the behavior of tissues. This emphasizes on nonlinear parameters extraction from hyperelastic characterization of tissues, which becomes a vital feature in classifying malignant from benign masses. In addition to that, large deformation could increase the operating strain range (15–30%) which further contributes to an increased signal to noise ratio (Samani et al., 2003).

Only few works are being reported in nonlinear stress strain characterization of tissues. Skovoroda et al. (1995) recognized the importance of nonlinear imaging and they evaluated nonlinear properties of tissues with the assumption of homogeneous material properties. Preliminary work on the measurement of hyperelastic parameters and fitting the models to experimental data were available in Samani et al. (2003), Mehrabian and Samani (2008), and O'Hagen and Samani (2008). Samani et al. (2003) modeled the stress strain response using a nonlinear hyperelastic constitutive relation of breast tissues in the form of a polynomial strain energy function. Oberai et al. (2009) applied a nonlinear hyperelastic model of breast tissue in vivo to estimate nonlinear metrics describing the tissue behavior. In reality, a soft tissue at larger strain may become stiff and might be seen as cancerous tissue by the radiologist. Hence understanding the nonlinear parameters of both normal and abnormal tissues become necessary but it is practically impossible to characterize the hyperelastic properties of normal tissues in vitro. In vivo characterization also needs certain calibration to ensure the repeatability. This leads to nonlinear stress strain characterization of tissue mimicking phantoms which are essential to study the nonlinear strain patterns of tissue. Pavan et al. (2010) characterized nonlinear properties of oil in gelatin agar phantoms where the contribution of agar in the phantom is small (0.58–2.81%).

Many ailments of the body have been observed to change the elastic properties and also viscous behavior (Taylor et al., 2001; Sridhar et al., 2007) of biological soft tissues. One challenge is to reproduce viscoelastic behavior in phantoms as observed in biological tissues. Mechanical response depends on the physiological and cellular microenvironmental process (Sridhar et al., 2007) of a specific patient. These changes can be detected by imaging viscoelastic features in combination with elastic features. Most of the biological tissues exhibit a time dependent stress strain behavior that is the characteristics of viscoelastic materials (Fung, 1993). A series of rheological tests on pig kidney have been performed to characterize its viscoelastic behavior of stress strain curves (Nasseri et al., 2002).

Recently many elastography related imaging techniques use dynamic shear modulus as the parameter for differentiating normal and cancerous lesions. Acoustic Radiation Force Impulse Imaging (Fatemi and Greenleaf, 2000; Walker et al., 2000; Nightingale et al., 2002) uses acoustic radiation force to generate images of the mechanical properties of soft tissues. The estimation of dynamic shear modulus is based on the measurements of speed of shear waves. The literature available on the measurement of dynamic shear modulus is limited. The mechanical behavior of breast and prostate tissue samples under dynamic compressive loading have been investigated in Krouskop et al. (1998). The imaging of viscoelastic properties of gelatin hydrogels and breast tissues was attempted in Sridhar et al. (2007). The measurement of viscoelastic properties of polyvinyl alcohol phantoms using diffusion wave spectroscopy was presented in Devi et al. (2005). Previous studies on agar based phantoms were reported in Nayar et al. (2011) in which viscoelastic properties at higher frequency range (25–100 Hz) and nanometer displacement were presented. However, in ultrasound

elastography, radiologist gives slight compression (less than 5%) by pressing the transducer probe. In addition to that, displacement is estimated by ultrasound time delay estimation methods where displacement in the millimeter range is easily traceable and preferable than nanometer.

Our work attempts to characterize linear elastic, viscoelastic and hyperelastic parameters of agar based phantoms which could be useful in stiffness investigating methods irrespective of their operating region either linear, nonlinear or viscoelastic. The focus of this work is to investigate the biomechanical properties of agar samples. The objectives are three fold.

- To investigate the linear elastic properties of tissues, linear stress strain characteristics of agar samples are studied by measuring the small strain (less than 4%) elastic properties of phantom samples. In this part of the work, phantom is assumed to exhibit linear elastic behavior. Using Hooke's law, elastic behavior of phantoms can be characterized by its Young's modulus.
- To measure the nonlinear characteristics of phantom material which provides insight into tissue stress strain curve nonlinearities. Here, common hyperelastic models namely Neo-Hookean, Mooney Rivlin (Mooney, 1940; Rivlin and Saunders, 1951), Ogden (Ogden, 1974) and Veronda Westmann (Veronda and Westmann, 1970) models are fitted from which the hyperelastic parameters are extracted which could be imaged using nonlinear elastography.
- To study the viscoelastic behavior of phantom samples by subjecting the samples to sinusoidally varying shear strains.

Here we report biomechanical properties of agar based samples for a wide range of agar concentration from 1.7% to 6.6%. In addition to hyperelastic modeling, we propose a method to extract stress difference at two different strain levels which is used to characterize the nonlinearity in a stress strain curve. This study could lead to a better understanding of biomechanical properties of human tissues and selection of optimum mechanical properties of both normal and cancerous tissues to do clinical diagnosis with great confidence. A complete database which provides biomechanical properties of normal and cancerous tissues is the need of the hour.

The paper is structured as follows: In Section 2, we present a phantom preparation procedure, the details about the instrument and experiment protocols followed. In Section 3 we present biomechanical characterization of phantoms. We also compare the parameters with values published in the previous literature for human tissues. Finally we present elastography images which we obtained for heterogeneous phantoms with embedded inclusions.

2. Materials and methods

2.1. *Preparation of tissue mimicking phantoms*

Agar is a common tissue mimicking material which is utilized in medical imaging. It is a gel formed by polysaccharide. The main focus of this paper is preparing and characterizing phantoms for ultrasound elastography imaging. We chose agar as the base of our phantoms due its near linear response of attenuation to ultrasound frequency ($f^{1.01}$) (Browne et al., 2003). Agar phantoms can be stored in distilled water for longer duration (more than 3 months) without variation of their acoustic and mechanical properties (within a tolerance 1–2%) due to water loss (Manickam et al., 2014).

The components of phantom sample are agar, N-propanol and deionized water. N-propanol was added to get the speed of sound in phantoms to be matched with human tissue (1540 m/s). Samples were made by varying concentration of agar from 2 g to 12 g in 100 ml of water (Kavitha and Ramasubba Reddy, 2012). Sample above 8 g was too stiff to be tested due to the brittle nature of agar at higher concentration. Hence we restricted our study on samples from 2 g to 8 g agar (1.7–6.6% w/w). Ingredients in the required proportions were mixed and stirred at room temperature until they were completely dissolved in deionized water. The mixture was heated in a microwave oven up to 90 °C, since the boiling point of agar is 85 °C. When the solution reached the boiling point, it was removed from the oven and allowed to cool at room temperature while being stirred at 1000 rpm using a magnetic stirrer. When the temperature of the solution reached 50 °C, it was poured into a cylindrical perspex mould. The solution in mould was allowed to settle down at room temperature for at least 12 h. Then the sample was unmoulded and stored in a fridge to avoid dehydration. The sample was taken out from the fridge and allowed to reach room temperature before doing any measurement. Two types of phantom samples were prepared for measurements (Fig. 1). The samples included in the compression test were cylindrical in shape with 38 mm diameter and 70 mm height. For rheological measurements, the sample was like a disc and having diameter 25 mm and thickness 1–2 mm.

2.2. *Quasi-static compression test*

The elastic properties of the agar samples were tested by a computer controlled electro-mechanical Universal Testing Machine (UTM) (*Jinan TE, China*). The 50 kN machine is equipped with an extensometer with 50 mm gauge length. Load cell measures test load and deformation of the specimen is measured by an elastometer. Samples were made such that its height is less than twice of its diameter to avoid the buckling effect. Quasi-static compression test was performed under displacement controlled mode (close loop). The load was applied under a strain rate of 0.5 mm/min up to a maximum of 15% strain and then it was unloaded in a similar way. Typically all samples were preconditioned for 5 s and preloaded to 1% of strain (0.7 mm). Compression above 15% of strain was tried which leads to a breakdown of the samples due to brittle nature of agar. Measurements were made for five sets of each category of samples at three different times. It is shown that mechanical parameters tend to increase during gelation (de Korte et al., 1997), so all tests on samples were performed after 12 h of storage.

2.3. *Elastic characterization*

Young's modulus is calculated from the slope of the linear portion of the loading curve using the least square fit. The

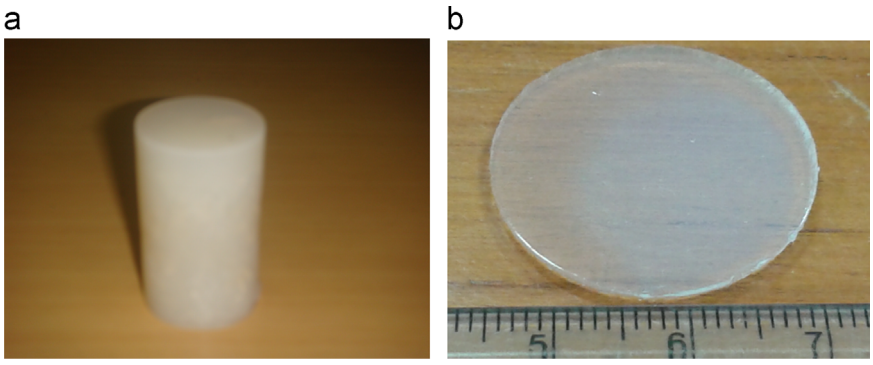

Fig. 1 – Prepared phantom samples (a) cylinder for elastic parameter measurement and (b) disc for viscoelastic properties measurement.

formula is

$$E = \frac{F/A}{\delta l/l} \tag{1}$$

where E is Young's modulus (kPa), F is the force applied to the object (N), A is the original cross section area through which force is applied (m^2), δl is the change in length (m), l is the original length of the sample (m). Measurements were done for all sets of samples and repeatability was ensured.

Polymers like agar and polyacrylamide as well as tissue samples are nonlinearly elastic in nature (Pavan et al., 2010) and the nonlinear behavior is represented by a hyperelastic model. A material is said to be hyperelastic if there exists a strain energy density function W that is a scalar function of one of the strain (deformation tensors), whose derivative with respect to a strain component determines the corresponding stress component. Assume a reference position vector X_i and a current position vector, x_i, the two are related by the displacement vector u_i, such that

$$x_i = X_i + u_i \tag{2}$$

In differential form,

$$dx_i = \frac{\partial x_i}{\partial X_j} dX_j = F_{ij}\, dX_j \tag{3}$$

where F_{ij} is the deformation gradient tensor. The right Cauchy–Green tensor is obtained from deformation gradient such that

$$C_{ij} = F_{mi}F_{mj} \tag{4}$$

Given the principal stretches at any deformation state of a material point as λ_1, λ_2, λ_3 and the strain invariants are defined as

$$I_1 = \text{trace}(C) = \lambda_1^2 + \lambda_2^2 + \lambda_3^3 \tag{5}$$

$$I_2 = \tfrac{1}{2}\left[(\text{trace}(C))^2 - \text{trace}\left(C^2\right)\right] = \lambda_1^2\lambda_2^2 + \lambda_2^2\lambda_3^2 + \lambda_1^2\lambda_3^2 \tag{6}$$

$$I_3 = \det(C) = \lambda_1^2\lambda_2^2\lambda_3^2 \tag{7}$$

For incompressible material, under uniaxial study,

$$\lambda_1 = \lambda; \quad \lambda_2 = \lambda_3 = \frac{1}{\sqrt{\lambda}}, \tag{8}$$

where λ, the stretch ratio, is defined as

$$\lambda = (L + \delta L)/L \tag{9}$$

in which L is the sample length at zero percent strain. The second Piola–Kirchhoff stress tensor S is given as

$$S = \frac{\partial W}{\partial E} = 2\frac{\partial W}{\partial C} \tag{10}$$

where E is the Green–Lagrange strain tensor. The Cauchy stress σ can be represented by E and F which can be written in terms of λ and W, respectively. For further understanding of equations readers are referred to Humphrey (2004). The stress equation in terms of stretch is further used for fitting the experimental curve and for identifying the model parameters.

Selection of such a strain energy density function is unlimited and arbitrary. Erkamp et al. (2004) used the Mooney Rivlin model to extract hyperelastic parameters of agar and gelatin phantoms for one set of stiffness sample. The Veronda Westmann model was used in biological nonlinear modulus constructions by Oberai et al. (2009). In this part of work, we present some of the well established and frequently employed hyperelastic models. Neo-Hookean, Mooney Rivilin, Veronda Westmann and Ogden models were fitted to stress strain data of four different stiffness phantoms to characterize the nonlinearity. The model parameters are reported and compared.

Neo-Hookean (NH) is the simplest hyperelastic model which is the reduced version of the Mooney Rivlin model. The strain energy density is given by the following equation:

$$W = C_{10}(I_1 - 3) \tag{11}$$

where C_{10} is the material constant which is related to shear modulus. For isotropic and incompressible materials, using uniaxial data the stress and stretch are related by the Neo-Hookean model which is

$$\sigma = 2C_{10}(\lambda^2 - \lambda^{-1}) \tag{12}$$

Small strain shear modulus μ is given by $2C_{10}$.

Mooney Rivlin (Mooney, 1940; Rivlin and Saunders, 1951) is the material model to represent incompressible, isotropic and elastic materials. The strain energy density function for an incompressible Mooney Rivlin two parameter model is

$$W = C_{10}(I_1 - 3) + C_{01}(I_2 - 3) \tag{13}$$

where C_{10} and C_{01} are the material constants for a 2 parameter model which are determined empirically. For consistency with linear elasticity, in the limit of small strain (less

than 4%), it is necessary that

$$\mu = 2(C_{10} + C_{01}) \tag{14}$$

where μ is the shear modulus. Once this function is determined i.e. C_{01} and C_{10} have been fit from the appropriate data, the hyperelastic material model is defined. The stress equation for two the parameter Mooney Rivlin material (Mooney, 1940; Rivlin and Saunders, 1951) can be formulated as

$$\sigma = 2C_{10}(\lambda - \lambda^{-2}) + 2C_{01}(1 - \lambda^{-3}) \tag{15}$$

The Veronda Westmann (VW) model (Veronda and Westmann, 1970) is similar to the Mooney–Rivlin model which also uses an uncoupled deviatoric dilatational strain energy. The dilatational term is identical to the one used in the Mooney–Rivlin model. The VW model can be used to describe certain types of biological materials that display exponential stiffening with increasing strain. It has been used to describe the response of skin tissue (Veronda and Westmann, 1970). Most of the cancer tissues are stiffer than the normal tissue and the stiffness varies nonlinearly. The Veronda Westmann model was popularly used to model the nonlinear behavior of breast tissues (Oberai et al., 2009). The VW model involves two material parameters and they are shear modulus of the material at zero strain, denoted by μ_0 and the nonlinear parameter γ, which denotes the nonlinearity of the material. μ determines the slope of the stress strain curve similar to Young's modulus and γ determines the rate at which the curve departs from linear behavior. The prepared phantoms have good agreement with breast tissues in the linear elasticity regime (Krouskop et al., 1998). In order to test the feasibility of the phantoms as a substitute for breast tissue in the hyperelasticity region, in this work the VW model was fitted to stress strain characteristics of the prepared phantom samples. Strain energy density W is given as

$$W = \mu_0 \left(\frac{e^{\gamma(I_1 - 3) - 1}}{\gamma} - \frac{I_2 - 3}{2} \right) \tag{16}$$

The stress and strain are related by the following equation in the Veronda Westmann model:

$$\sigma = 2\lambda^2 \mu_0 e^{\gamma(\lambda^2 - 2\lambda^{-1} - 3)} - \frac{2}{\lambda}\mu_0 e^{\gamma(\lambda^2 - 2\lambda^{-1} - 3)} + \frac{\mu_0}{\lambda^2} - \mu_0 \lambda \tag{17}$$

The Ogden model (Ogden, 1974) which is popularly used to fit isotropic biological tissue was also fitted for the stress strain curve of the prepared samples. Ogden strain energy function is written in terms of principal stretches instead of the invariants. Ogden form can be reduced into Neo-Hookean and Mooney–Rivlin by choosing particular values for α and N. Ogden form of strain density function W is given by

$$W = \sum_{r=1}^{N} \frac{\mu_r}{\alpha_r} \left(\lambda_1^{\alpha_r} + \lambda_2^{\alpha_r} + \lambda_3^{\alpha_r} - 3 \right) \tag{18}$$

where $N = 1,2,3,\ldots$ and μ_r and α_r are constants. The initial shear modulus is given as $2\mu = \sum_{r=1}^{N} \mu_r \alpha_r$. For incompressible, isotropic material under uniaxial study, the Cauchy stress for the Ogden model $N = 1$ is

$$\sigma = \mu_1 (\lambda^{\alpha_1} - \lambda^{-\alpha_1/2}) \tag{19}$$

The large displacement data from the uniaxial compression test was given as input to curve fitting algorithms. Hyperelastic model parameters were estimated by fitting the model equations (12), (15), (17) and (19) to the experimental stress strain data using nonlinear least squares with the Levenberg Marquart algorithm in Matlab. Since the ANSYS curve fitting toolbox has built in tool to characterize the parameters for Neo-Hookean, Mooney Rivlin and Ogden models, results were also verified by fitting the models to data using ANSYS.

2.4. Viscoelastic characterization

The viscoelastic behavior of biological tissues can be measured by applying a periodic compressive or shear displacement to a cylindrical sample of uniform thickness and cross sectional area and measuring the force response (Fung, 1993; Zhang et al., 2007). If the viscoelastic behavior is linear, the strain will also alternate sinusoidally but will be out of phase with stress. The complex shear modulus is given by

$$G^* = G' + iG'' \tag{20}$$

The real part of the complex modulus (G') is known as storage modulus, as it is an indicator of the materials ability to store energy. The imaginary part (G'') is known as the loss modulus, related to the amount of energy lost through the viscous process.

In this part of viscoelasticity measurement, two different types of dynamic tests operating in the frequency domain were performed using a rheometer set up (*Model Physica MCR 301, Anton-Paar Germany*). The sample was placed on the sample base and parallel plate geometry (PP25) was used for the measurement so as to ensure uniform loading and prevent sample buckling. The experiment protocol is as follows.

Amplitude sweep oscillatory test: Using a strain controlled rheometer, the samples were subjected to a sinusoidal deformation at a fixed frequency of 1 Hz. The strain amplitude was increased from 0.01% to 25% large oscillatory deformation at a precompression level of 2%, 3%, 5% and 10% applied on samples after preconditioning for 5 s. The amplitude sweep test was conducted to find out the linear viscoelastic region (LVER) of the samples which explains about the sample behavior for various application of strain. From the result, stress or strain within the LVER is selected and incorporated into linear elastogram application. Cancer exhibits greater nonlinearity i.e. the change in elastic modulus with strain is greater than the change observed in normal tissues. Moreover elastic modulus of tissue is not constant and depends on precompression applied. To investigate this, storage modulus values for various applied strain at different precompression levels is analyzed.

Frequency sweep: Using the rheometer, the storage and loss modulus G' and G'' were obtained as a function of frequency. Frequency was increased from 0.1 Hz to 5 Hz. The strain was fixed at 3% strain for (2 g and 4 g) and 1% strain for 6 g and 0.2% strain for 8 g which are within the linear viscoelastic region.

The rheometer head initially moved down towards the sample at a pre-programmed user defined velocity (1 μm/s) and reached the specified precompression level. The rheometer set up also consists of a normal force sensor capable of measuring the normal force i.e. the range of 0.01–50 N with a resolution of 0.002 N. The tip of the loading arm and sample base were properly cleaned before placing the sample. Initial calibration was done to attain zero gap. Sample was

preconditioned at an initial contact level for 5 s then required precompression was given using a normal force loading arm. Having completed all these steps, shear oscillatory force was given as per the experiment protocol. Around 10–15 samples were prepared from the same stock solution for each category of phantom. A fresh sample was used for each experiment, in order to avoid any time history dependent effects of viscoelasticity.

3. Results and discussion

In order to perform ultrasound elastography imaging, the prepared samples do mimic soft tissues in terms of acoustic and mechanical properties. The acoustic parameters such as acoustic velocity, attenuation coefficient and acoustic impedance were measured using the pulse echo method at 5 MHz frequency (Manickam et al., 2014) and they match with human tissue (Table 1).

3.1. *Linear elastic characterization*

Uniaxial compression test was conducted and stress strain values were recorded. From the recorded data, stress and strain relationship of the phantom under uniaxial loading was plotted (Fig. 2) and Young's modulus was calculated from the initial linear region (up to 4% of strain) of the curves using least square fit (Fig. 3). The total range of elastic moduli achieved by varying the agar concentration from 2 g to 8 g is 50–450 kPa which covers the entire range of normal and abnormal tissue stiffness (Fung, 1993; Krouskop et al., 1998).

3.2. *Hyperelasticity characterization*

If we consider the stress strain curve of agar sample (Fig. 4), it can be categorized into two regions. One is a linear elastic region (at the initial portion of the curve) and the second one is a hyperelastic region where the material exhibits more stress for a small increment in strain. Nonlinear elastography is intended to operate in the second area of the stress strain curve and it is hypothesized that the classification accuracy of different types of tumor could be improved if we consider the nonlinear elastic parameters. To have a good understanding of tissue nonlinearities, we are in need of a phantom which has similar characteristics to that of tissues.

For the recorded data from uniaxial compression experiment, Neo-Hookean, Mooney Rivlin, Veronda Westmann and Ogden models were fitted and the results are shown with mean experimental stress strain data in Fig. 5 and the material parameters are shown in Table 3. Shear modulus at zero strain was calculated as per the procedure explained in Section 2.3. From that, Young's modulus at zero strain was calculated and it is comparable to the calculated Young's modulus of uniaxial test for small strain (less than 4%) (Table 3).

Table 1 – The mean and standard deviation values for acoustic properties of the prepared samples and human tissue (Ludwig, 1950; Hill et al., 2004).

Parameters	Human tissue	2 g agar sample	4 g agar sample	6 g agar sample	8 g agar sample
Sound speed ($m\,s^{-1}$)	1540	1564±88	1581±26	1571±12	1671±124
Attenuation ($db\,cm^{-1}\,MHz^{-1}$)	0.7	0.8268±0.755	0.6915±0.123	0.7802±0.003	0.7121±0.2313
Acoustic impedance ($kg\,m^{-2}\,s^{-1}$)	1.63×10^6	1.66×10^6±0.165	1.76×10^6±0.045	1.61×10^6±0.127	1.71×10^6±0.012

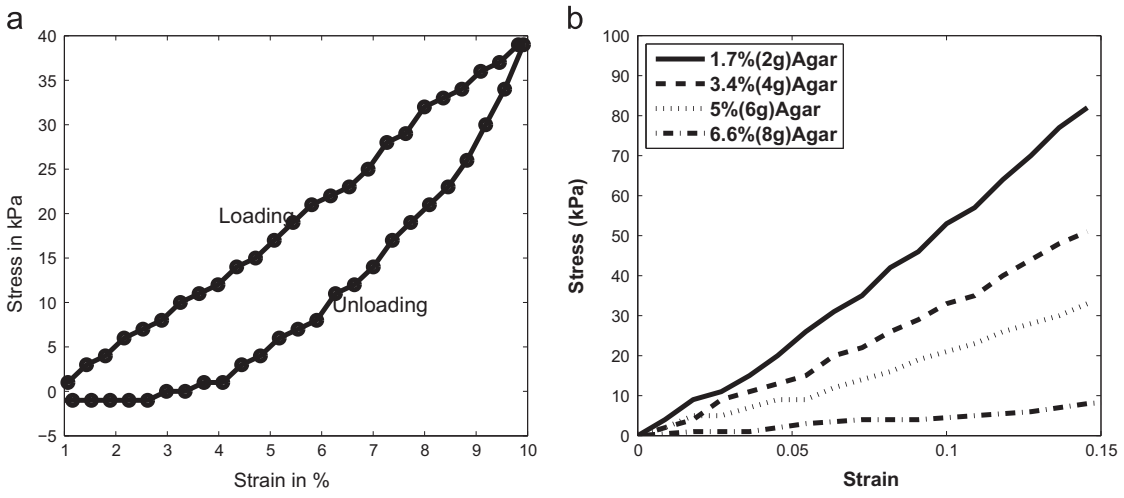

Fig. 2 – (a) A typical stress strain curve of agar sample. Notice that the curve has hysteresis which shows that the samples are viscoelastic in nature. For elastic characterization, loading part alone was considered. (b) Stress strain loading curve for samples from 1.7% to 6.6% of agar samples.

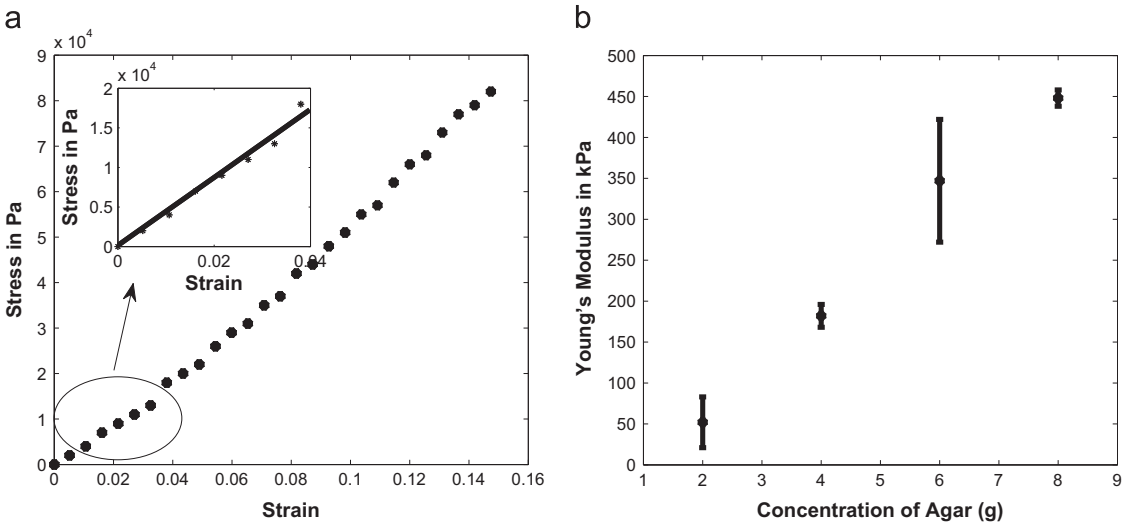

Fig. 3 – (a) Stress strain characteristics of 8 g sample. Linear region is fixed at the initial portion (4% of strain) and solid line shows the least square fit. (b) Mean and standard deviation of Young's modulus for various samples of agar concentration from 1.7% to 6.6%.

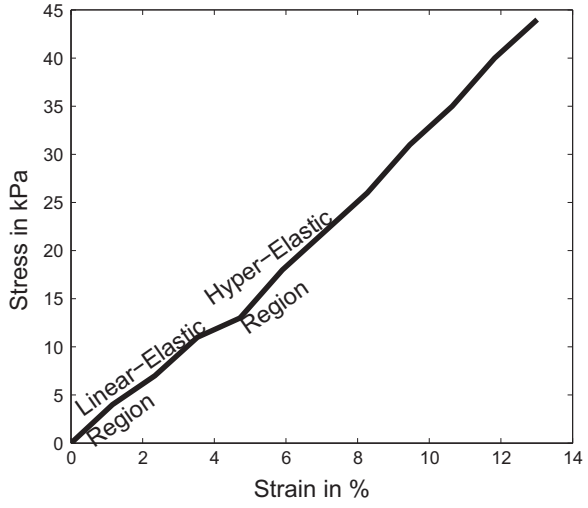

Fig. 4 – Typical stress strain curve of the phantom.

If we consider the result of Neo-Hookean model, the goodness of fit (R^2) is comparatively less than the other models. In the Mooney Rivlin model parameters, C_{01} which relates I_2 invariant is negative for all samples. If only one set of test data (uniaxial tension or compression) is used to determine the coefficients, there is a possibility that either C_{10} or C_{01} is negative (Subhani and Krishna Kumar, 2009). This leads to instability of the model in predicting equi-biaxial tension or compression test (Subhani and Krishna Kumar, 2009). Since we consider uniaxial study of isotropic material, the MR model could be used for fitting the experimental curve of the prepared samples. The two parameters μ_0 and γ of the Veronda Westmann model are calculated and listed in Table 3. We can notice that when agar concentration increases, stiffness of the sample increases which is shown by the increase in μ_0. However, nonlinearity parameter γ shows almost constant trend which might indicate that an increase in agar concentration has no effect on nonlinearity in the stress strain curve. A similar kind of result was obtained by Pavan et al. (2010).

Our study combines some of the popular and established hyperelastic models for characterizing constitutive relations of agar based phantoms and reports the parameters. The reported parameters could be used as inputs in finite element hyperelastic simulation of phantoms and modeling of tissue. Commercial finite element software offers some of the models as built in models. Users can select the model based on their requirement and the reported data will serve as an input tool for the simulation of composite phantoms.

We tried to extract the nonlinearity of the stress strain curve using incremental differential Young's modulus. Young's modulus is constant only in the linear stress strain region. The studies reported that Young's modulus becomes strain dependent parameter at higher strain level, where tissue becomes stiff. Malignant masses become stiffer more rapidly than benign masses while increasing the applied strain. Considering a 2 g agar sample as healthy tissue and the other three samples are representations of cancerous tissue (Krouskop et al., 1998), we propose a classification scheme (Fig. 6) by computing the stress difference offered by these samples at two strain levels. The stress difference between the three samples to the 2 g sample becomes more significant at higher strain (above 10%). This behavior is more prominent for high modulus contrast samples (in which modulus contrast of inclusion to the background is greater than 10 dB), since they exhibit strong nonlinear stress strain behavior. This can be used as a feature to differentiate benign which are low modulus contrast inclusions in which modulus contrast of the inclusion to the background is less than 10 dB from malignant lesions (high modulus contrast lesions) of human body tissue. If $\delta\sigma_{23} \gg \delta\sigma_{13}$ represents the malignant tissue and $\delta\sigma_{22} \geq \delta\sigma_{12}$ and $\delta\sigma_{21} \geq \delta\sigma_{11}$ represent benign nature of tissue where $\delta\sigma_{ij,i=1,2}$ represents the strain level and $j=1,2,3$ represents 4 g, 6 g and 8 g phantoms with respect to 2 g respectively.

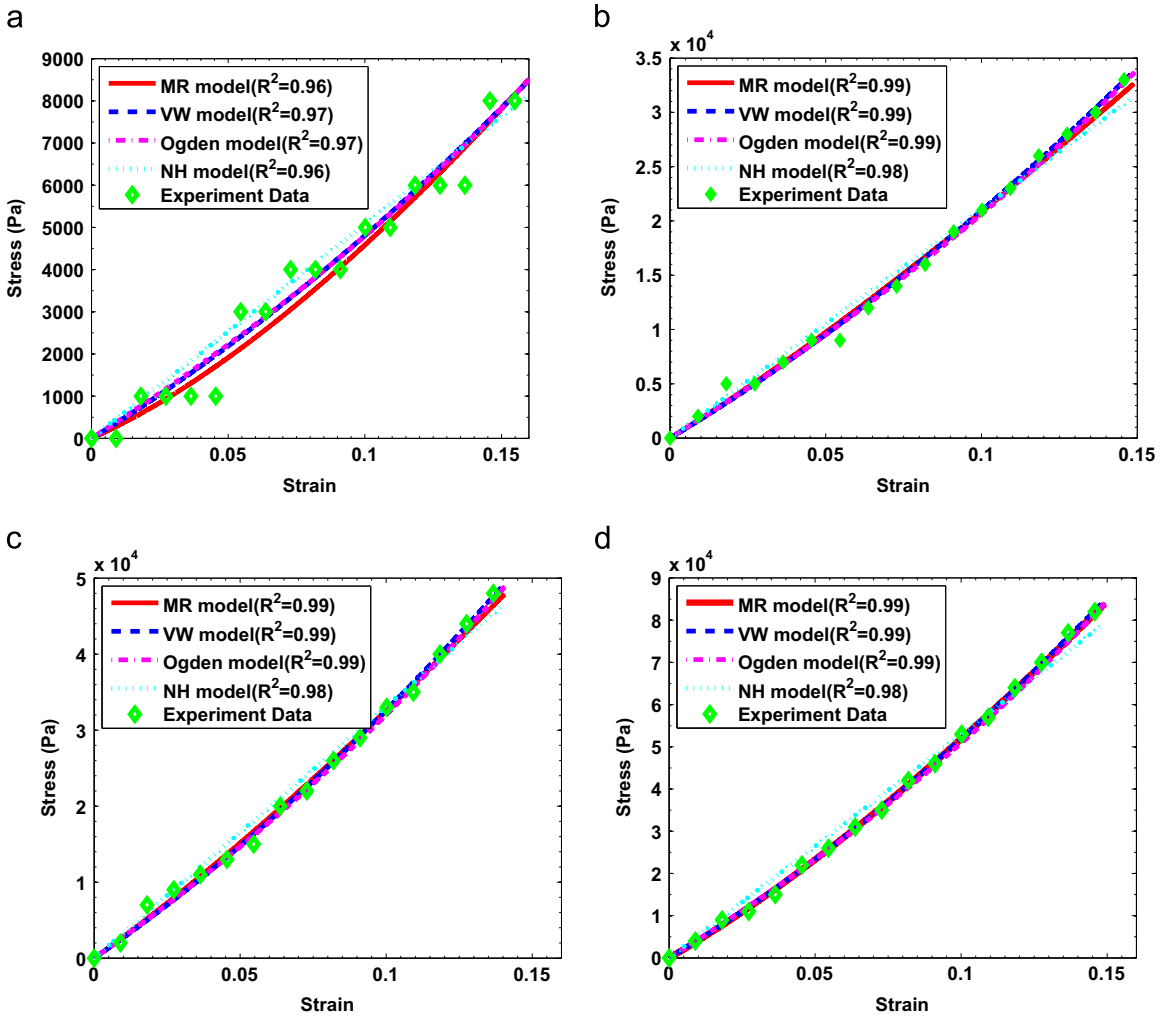

Fig. 5 – (a–d) Neo-Hookean (NH), Mooney Rivlin (MR), Ogden and Veronda Westmann (VW) models are fitted to experimental stress strain data for 2 g, 4 g, 6 g and 8 g samples respectively.

The samples used for mechanical testing was cylindrical in shape and they did not change their volume during testing. However the incompressibility assumption of the prepared samples was tested using an ultrasound technique. The longitudinal wave velocities for all the samples were measured and they are in the range from 1564 to 1671 m/s (Manickam et al., 2014). Similarly we measured the shear wave velocities and they are in the range 1.5–8 m/s. Using the formula

$$\nu = \frac{1-2\left(\frac{V_T}{V_L}\right)^2}{2-2\left(\frac{V_T}{V_L}\right)^2} \tag{21}$$

the Poisson's ratio ν was calculated and they are in the range 0.42–0.5 which ensures the incompressibility condition.

3.3. *Viscoelastic characterization*

The results of frequency sweep shear oscillation test for two samples at 3% strain are shown in Fig. 7. It shows the measured variation in the storage and loss modulus with frequency over the range 0.01–5 Hz for two different agar concentrations with strain amplitude of 3% applied on the sample.

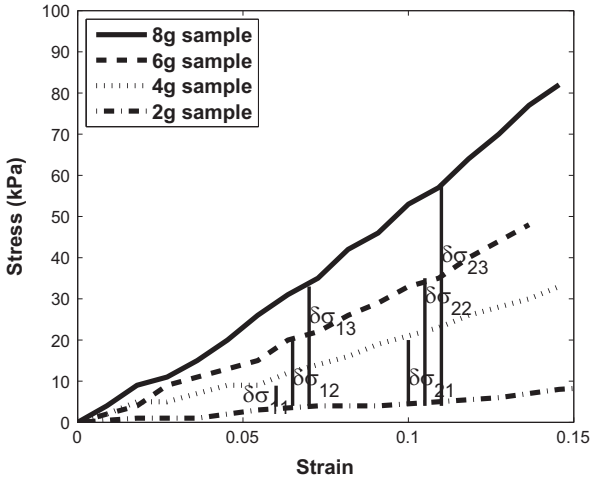

Fig. 6 – Stress strain curve of all the samples with stress difference parameter at two strain levels.

There is no noticeable variation in storage and loss modulus with frequency. The storage modulus is always (around 20 times) larger than the loss modulus for all frequencies. This is similar to

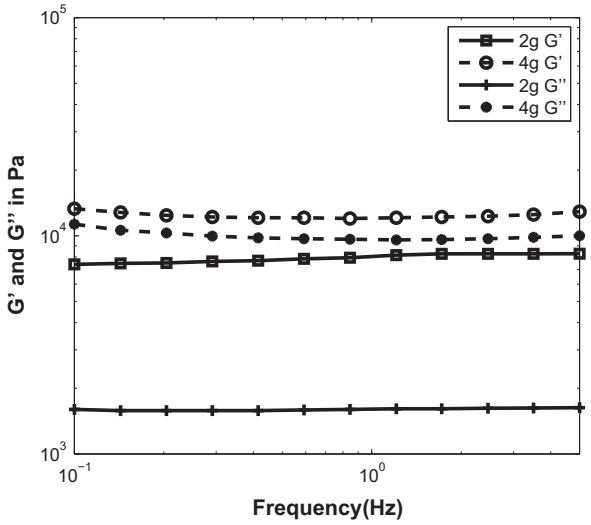

Fig. 7 – Variation of storage and loss modulus of 2 g and 4 g samples at frequencies (from 0.1 to 5 Hz). Note that storage modulus is always higher than loss modulus.

the behavior of biological tissues (Krouskop et al., 1998; Zhang et al., 2007). It is observed that loss modulus values are uniformly lesser than 30 kPa which represents low frequency damping of agar samples and this result matches with the one reported in Nayar et al. (2011).

The results of amplitude sweep for samples with initial and precompression are shown in Fig. 8. As agar concentration increases, there is a significant increase in both the moduli. Thus the prepared samples cover both normal and pathological conditions. In addition to that, the linear viscoelastic region (LVER) under which the storage and loss modulus are independent of strain is also reduced for higher concentration agar samples (above 4 g). The above observation holds good even for loading with higher frequencies 100–200 Hz (Nayar et al., 2011).

Nasseri et al. (2002) conducted a series of shear tests to find out the viscoelastic properties of pig kidney and reported that kidney has a linear viscoelastic limit at a strain approximately of 0.2%. The same kind of trend is observed for 8 g phantom which had a similar LVER limit. In order to compare the results obtained from shear oscillatory tests in

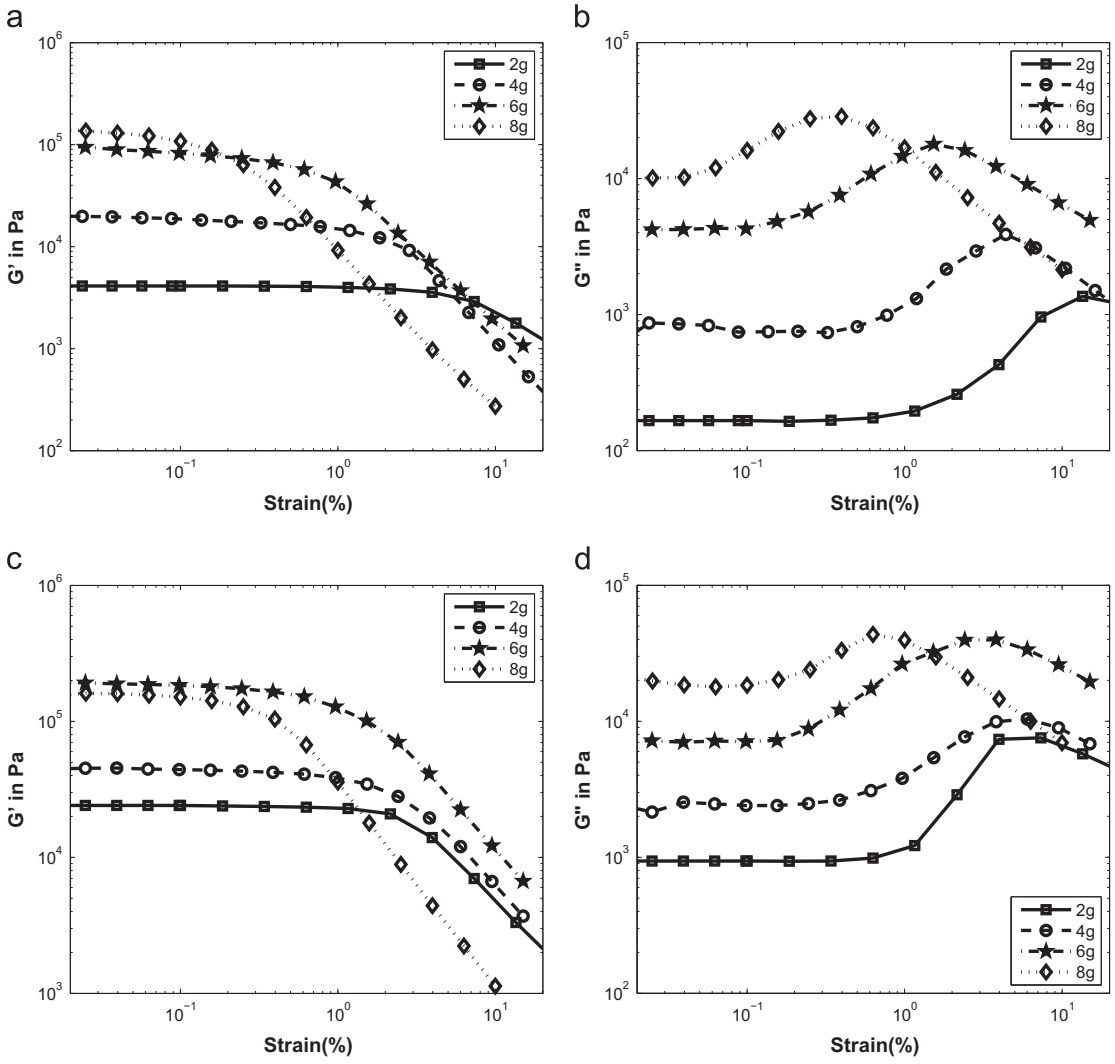

Fig. 8 – Strain sweep oscillation experiment of four sets of samples (top) at an initial compression level to have bare contact (bottom) at precompression level 5% (2 g and 4 g) and 2% (6 g and 8 g). (a) and (c) show storage modulus and (b) and (d) show loss modulus. We can notice the linear viscoelastic limit. G' and G'' reduce significantly when strain exceeds the linear limit. Notice that, for an increase in agar concentration, storage modulus increases whereas width of the linear viscoelastic region decreases.

linear and nonlinear regions, the oscillatory test was conducted at strain amplitude of 2% which is higher than 0.2% at the same frequency of 1 Hz for 8 g sample. We note that, G′ is less than G″ and these are independent of frequency variation which is also comparable with Nasseri et al. (2002).

Fig. 9 presents the mean and standard deviation of shear modulus of samples with different agar concentration at an initial contact (without compression) and 2–5% precompression levels. At low agar concentration (2–4 g) there is no significant variation in modulus at two compression levels. At higher agar concentration (above 4 g) there exists large variations in modulus values at the two precompression levels. A similar behavior was observed for breast tissue (Table 2) (Krouskop et al., 1998). This justifies the suitability of developed agar phantoms for elastography applications more specifically for breast and prostate cancer applications. The phantom could be used as a versatile platform in linear, nonlinear elastic and viscoelastic applications. The measured overall parameters are presented in Table 3. Elastic modulus at the linear region, elastic modulus at zero strain calculated from hyperelastic parameters and Young's modulus calculated from viscoelastic shear modulus of all the samples are comparable and have good agreement among themselves.

It is well known that tumor tissues are stiffer as well as nonlinear than normal tissues. The biomechanical properties with which stiffness imaging is being operated must characterize both qualities i.e. increased stiffness and nonlinearity. From the results, we can notice that shear storage modulus and range of LVER could be identified as optimum features for in vivo investigation. Galaz et al. (2009) have demonstrated that axial shear strain images are useful than axial compressive strain images. In elastography, if dynamic shear modulus and nonlinearity of shear modulus are imaged, it would give unique diagnostic information. The prepared phantoms report, good dynamic shear properties and a clear distinguishable LVER region for different stiffness categories. It also provides the users more flexibility in controlling the parameters like agar concentration, precompression, LVER and applied strain. In future, if the nonlinear viscoelastic properties of these samples are characterized by analyzing the harmonics of stress and strain oscillatory data, it may give very unique image pattern which would increase the specificity of stiffness imaging methods still better.

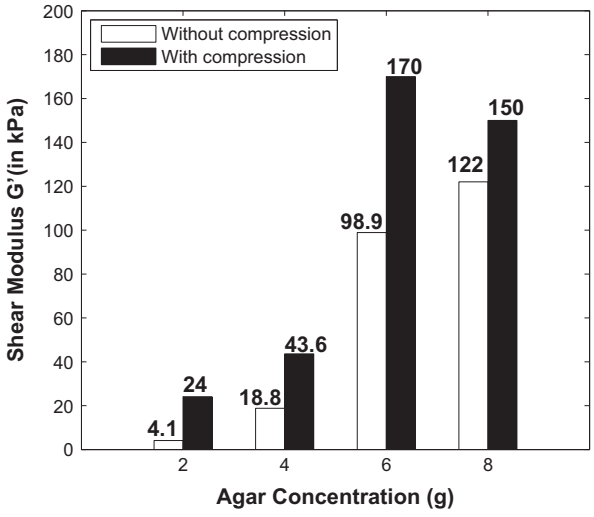

Fig. 9 – Shear modulus of four sets of samples with concentration (2,4,6,8) g agar. White color bar represents modulus measured at minimal compression to maintain contact and black color bar represents modulus measured at a precompression of 2–5%.

Conventional ultrasound B-mode image and elastogram of inclusions which represent two different classes of cancer (malignant and benign) are presented in Fig. 10. Elastogram was acquired from a commercially available scanner, namely, Siemens S2000 ACUSON Antares (Siemens, Erlangen, Germany). The inclusion in Fig. 10(a) is not clear in B-mode. But it is clearly visible in elastography. The low modulus contrast inclusion (modulus contrast less than 10 dB) of Fig. 10(b) is also clearly differentiable from the surroundings in the elastogram. The images also show the extent of the resolution available from elastography. Further developments of similar heterogeneous phantoms may allow the clinicians to more accurately mimic healthy and pathological soft tissues for ultrasound elastography.

4. Conclusion

In this paper, agar based homogeneous tissue mimicking phantoms catering to normal and pathological biological tissues were developed for ultrasound elastography imaging for various concentrations of agar from 1.7% to 6.6% by weight. We hypothesize that an increase in agar concentration results in an increase in stiffness (either Young's modulus or Shear modulus) as well as an increase in nonlinearity. To test the hypothesis, we conducted a uniaxial compression test on the prepared samples up to 15% of strain using a universal testing machine in displacement control mode and deduced the stress strain characteristics which show hysteresis and nonlinearity. Assuming that the phantoms are elastic and considering the loading part of the stress strain curve, Young's modulus values were computed for small strain (<4%). They are in the range from 50 kPa to 450 kPa

Table 2 – Comparison of elastic moduli of the developed phantoms with biological tissues.

Phantom sample	Closely matching human tissue	Elastic modulus (kPa)	Compression level
2 g	Normal breast	12–72	Initial-5%
4 g	Normal prostate	56.4–130.8	Initial-5%
2 g	Normal Liver	12–40	Initial-2%
6 g and 8 g	Breast and prostate cancerous tissue	56–450	Initial-2%

Table 3 – Summary of material model (linear elastic, hyperelastic and viscoelastic parameters for various agar concentration).

Quasi-static small and large strain and dynamic loading summary					
Method	Prepared samples	2 g agar	4 g agar	6 g agar	8 g agar
Quasi-static small deformation	Young's modulus (kPa)	52±31	182±14	347±75	448±10
Quasi-static large deformation hyperelastic model	*Neo-Hookean* (kPa)				
	C_{10}	8.4±0.9	35±0.2	55±1.6	88±1.2
	$E=6C_{10}$	50.4	210	330	528
	Mooney Rivlin (kPa)				
	C_{10}	43.73±0.12	122.7±8	196.8±7.8	377±10.2
	C_{01}	−38.89±1.3	−93.065±3.2	−151±4.7	−310.55±7.88
	$E=6(C_{01}+C_{10})$ (kPa)	29.04	177.8	274.8	398.7
	Veronda Westmann				
	μ_0 (kPa)	22.7±1.5	97.28±3.12	159.6±5.78	264.9±6.78
	γ	0.05962±0.0023	0.0576±0.0014	0.06383±0.0134	0.06889±0.089
	$E=3\mu_0$ (kPa)	68.1	291.84	478.8	794.7
	Ogden				
	μ_1 (kPa)	4.4±1.1	18±1.12	26±3.87	41±2.78
	α_1	6.3±1.2	6.6±1.4	7±1.3	7.3±1.1
	$E=\frac{3}{2}\mu_1\alpha_1$ (kPa)	41.58	178.2	273	448

Dynamic frequency=1 Hz	Viscoelastic parameters (kPa)	2 g agar		4 g agar		6 g agar		8 g agar	
		Initial	5% comp.	Initial	5% comp.	Initial	2% comp.	Initial	2% comp.
	G'	4.12	24	18.8	43.6	98.9	170	122	150
	G''	0.166	0.938	0.854	2.5	4.22	7.01	10.2	21.9
	LVER (%)	5	2	2	1	1	0.6	0.2	0.1
	$E=3\mu$	12.36	72	56.4	130.8	296.7	510	366	450

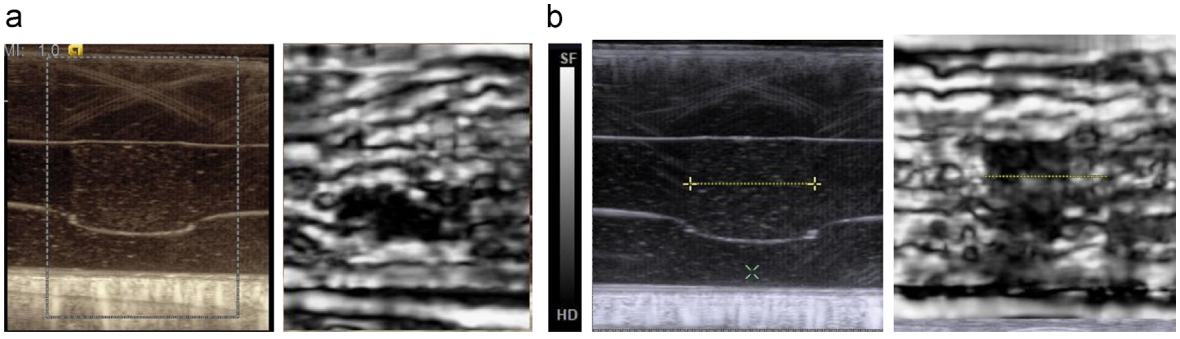

Fig. 10 – Ultrasound B-mode images (left) and linear elastograms (right) of a heterogeneous phantom prepared with 2 inclusions (8 g and 4 g agar) of height 1.5 cm and width 1 cm in a soft (2 g agar) background. (a) represents malignant and (b) represents benign lesion.

which are a similar range of normal and abnormal breast tissues. The suitability of the prepared samples for nonlinear elastography was examined by characterizing the nonlinearities present in the stress strain curve up to 15% of strain. Neo-Hookean, Mooney Rivlin, Veronda Westmann and Ogden models were fitted and hyperelastic parameters were computed for all types of samples. Young's modulus at zero strain were computed and they are comparable to small strain Young's modulus values. However, the nonlinearity parameter γ derived from the Veronda Westmann model shows less variation when agar concentration increased from 1.7% to 6.6%. We further analyzed the nonlinearity by computing stress difference at two different strain levels which could be used to differentiate the stiffness of inclusion. Hysteresis in

the stress strain curve indicates that the phantoms are viscoelastic in nature. The shear modulus were measured by conducting oscillatory rheometry at 0.1 Hz–5 MHz at pre-compression levels from 2 to 5%. The frequency sweep test shows that the storage and loss moduli values are not varying with the applied loading frequency. Storage modulus increases as well as LVER decreases when agar concentration increases from 2 g to 8 g and the results are enhanced when the precompression level is increased from 2% to 5%. This study combines all the mechanical properties and suggest that the prepared samples could be used in ultrasound elastography as versatile phantoms. Moreover, this study suggests that out of the measured parameters, dynamic shear modulus values are more promising in classification of stiffer inclusions based on their degree of stiffness and increased nonlinearity.

Acknowledgments

The authors would like to thank Dr. Abhijit Deshpande Department of Chemical Engineering and Dr. Arockia Rajan Department of Applied Mechanics, IIT Madras, for providing the facility and for help in doing the measurement, as well as Prof. C. Lakshmana Rao for valuable discussions and suggestions. Anonymous reviewers are gratefully thanked for their very thorough and inspiring review, which substantially improved the quality of the manuscript.

REFERENCES

Browne, J., Ramnarine, K., Watson, A., Hoskins, P., 2003. Assessment of the acoustic properties of common tissue mimicking test phantoms. Ultrasound Med. Biol. 29, 1053–1060.

de Korte, C.L., Cespedes, E.I., van Der Steen, A.F.W., Norder, B., Nijenhuis, K.T., 1997. Elastic and acoustic properties of vessel mimicking material for elasticity imaging. Ultrasonic Imaging 19, 112–126.

Devi, U.C., Vasu, R.M., Sook, A.K., 2005. Design, fabrication and characterization of a tissue equivalent phantom for optical elastography. J. Biomed. Opt. 10, 044020-1–044020-10.

Erkamp, R.Q., Emelianov, S.Y., Skovoroda, A.R., O'Donnell, M., 2004. Nonlinear elasticity imaging: theory and phantom study. IEEE Trans. Ultrasound Ferroelectron. Freq. Control 51, 532–539.

Fatemi, M., Greenleaf, J.E., 2000. Probing the dynamics of tissue at low frequencies with the radiation force of ultrasound. Phys. Med. Biol. 45, 1449–1464.

Fung, Y.C., 1993. Biomechanics: Mechanical Properties of Living Tissues. Springer-Verlog, New York, USA, pp. 243–312.

Galaz, B., Thitaikumar, A., Ophir, J., 2009. Axial-shear strain distributions in an elliptical inclusion model (Part I): a simulation study. In: Proceedings of the Eighth International Conference on the Ultrasonic Measurement and Imaging of Tissue Elasticity, p. 99.

Hill, C.R., Bamber, J.C., Haar, G.R., 2004. Physical Principles of Medical Ultrasonics. John Wiley and Sons, New York, USA93–186.

Humphrey, J.D., 2004. An Introduction to Biomechanics: Solids and Fluids, Analysis and Design. Springer, New York, USA, 271–287.

Kavitha, M., Ramasubba Reddy, M., 2012. Characterisation of tissue mimicking phantoms for acoustic radiation force impulse imaging. In: Proceedings of the IEEE International Conference on Imaging Systems and Technology (IST2012), Manchester, UK, pp. 553–557.

Krouskop, T.A., Wheeler, T.M., Kallel, F., Garra, B.S., Hall, T., 1998. Elastic moduli of breast and prostate tissues under compression. Ultrasound Imaging 20, 260–274.

Ludwig, G.D., 1950. The velocity of sound through tissues and the acoustic impedance of tissues. J. Acoust. Soc. Am. 22, 862–866.

Manickam, K., Machireddy, R., Seshadri, S., 2014. Study of ultrasound stiffness imaging methods using tissue mimicking phantoms. Ultrasonics 54, 621–631.

Mehrabian, H., Samani, A., 2008. An iterative hyper elastic parameters reconstruction for breast cancer assessment. In: Proceedings of SPIE, vol. 6916.

Mooney, M., 1940. A theory of large elastic deformation. J. Appl. Phys. 11, 582–592.

Nasseri, S., Bilston, L., Phan-Thein, N., 2002. Visco elastic properties of pig kidney in shear, experimental results and modeling. Rheol. Acta 41, 180–192.

Nayar, V.T., Weiland, J.D., Nelson, C.S., Hodge, A.M., 2011. Elastic and viscoelastic characterisation of agar. J. Mech. Behav. Biomed. Mater. 7, 60–68.

Nightingale, K., Bentley, R., Trahey, G., 2002. Observations of tissue response to acoustic radiation force: opportunities for imaging. Ultrasonic Imaging 24, 100–108.

O'Hagen, J.J., Samani, A., 2008. Measuring of the hyper elastic properties of tissue slices with tumor inclusion. Phys. Med. Biol. 53, 2257–2569.

Oberai, A.A., Gokhale, N.H., Goenezen, S., Barbone, P.E., Hall, T.J., Sommer, A.M., Jiang, J., 2009. Linear and nonlinear elasticity imaging of soft tissue in vivo: demonstration of feasibility. Phys. Med. Biol. 54, 1191–1207.

Ogden, R.W., 1974. Large deformation isotropic elasticity-on correlation of theory and experiment for incompressible rubber like solids. Proc. R. Soc. Lond. A 328, 567–583.

Ophir, J., 1991. Elastography: a quantitative method for imaging the elasticity of biological tissues. Ultrasound Imaging 13, 111–134.

Pavan, T.Z., Madsen, E.L., Frank, G.R., Carneiro, A.A.O., 2010. Nonlinear elastic behaviour of phantom materials for elastography. Phys. Med. Biol. 55, 2679–2692.

Rivlin, R.S., Saunders, D.W., 1951. Large elastic deformations of isotropic materials. VII. Experiments on the deformation of rubber. Philos. Trans. R. Soc. Lond. A243, 251–288.

Samani, A., Bishop, J., Luginbubk, C., Plewes, D.B., 2003. Measuring the elastic of ex-vivo small tissue samples. Phys. Med. Biol. 48, 2183–2198.

Skovoroda, R., Klishko, A., Gusakyan, D., 1995. Quantitative analysis of the mechanical characteristics of pathologically changed soft biological tissues. Biophysics 40, 1359–1364.

Sridhar, M., Liu, J., Insana, M.F., 2007. Elasticity imaging of polymer media. ASME Trans. J. Biomech. Eng. 129, 259–272.

Subhani, M.P., Krishna Kumar, R., 2009. A new stored energy function for rubber like materials for low strains. Mech. Adv. Mater. Struct. 16, 402–416.

Taylor, L.S., Richards, M.S., Moskowitz, A.J., Lerner, A.L., Rubens, D.J., Parker, K.J., 2001. Viscoelastic effects in sonoelastography: impact on tumor detectability. In: Proceedings of IEEE Ultrasonics Symposium, Atlanta, USA, pp. 1639–1642.

Veronda, D.R., Westmann, R.A., 1970. Mechanical characterization of skin-finite deformations. J. Biomech. 3, 111–124.

Walker, W.F., Fernandes, F.J., Negron, L.A., 2000. A method of imaging visco elastic parameters with acoustic radiation force. Phys. Med. Biol. 45, 1437–1447.

Zhang, M., Castaneda, B., Wu, Z., Priya, N., Joseph, J.V., Rubens, D.J., Parker, K.J., 2007. Congruence of imaging estimators and mechanical measurements of viscoelastic properties of soft tissues. Ultrasound Med. Biol. 33, 1617–1631.